Z. Physik B 36, 37–46 (1979)

01-79.03

Zeitschrift für Physik B

© by Springer-Verlag 1979

C. N. E. A. Biblioteca
ARCHIVO PUBLICACIONES
Nº 1 AÑO 1979

Intermediate Valence: Phase Diagram and Kondo Behaviour in a Simple Model

B. Alascio, H. Wio and A. López
Centro Atómico Bariloche*, Instituto Balseiro**, S.C. de Bariloche, R.N., Argentina

Received March 12, 1979

We have studied an infinitely narrow band version of the Anderson Hamiltonian. Including a Coulomb repulsion between localized and band states in the mean field approximation, we have been able to describe metal-insulator phase transitions and different properties characteristic of intermediate valence in both phases. These include: non-integer occupation, specific heat, saturating static magnetic succeptibility and dynamical properties such as Mössbauer spectra and spin flip neutron spectra. We discuss for what range of values of the parameters some results can be reproduced by a narrow band version of the Kondo Hamiltonian.

Introduction

There has been a considerable amount of theoretical effort in the past few years devoted to the understanding of intermediate valence systems [1]. Most of the theoretical models considered in the literature contain two more or less realistic correlated ionic configurations hybridized to a set of uncorrelated conduction-like states. The complexity of the problem has forced researchers in this area to make simplifying assumptions in order to keep the mathematics of the models tractable.

More recently, there have been efforts to treat the full *periodic* Anderson Model within the Hartree-Fock approximation [2]. The importance of this approach lies on the fact that it allows to describe intersite correlations and restores the periodicity to the eigenstates of the system. This gives some insight into those properties of homogeneous intermediate valence compounds which depend on intersite interactions. The price one has to pay for this is the neglect of all intra-site correlations.

In this paper we have adopted the complementary point of view, i.e. we reduced the problem to that of an aggregate of independent sites, where intra-atomic correlations and hybridization can be treated exactly. Equivalently we have assumed the conduction-like states to correspond to extremely heavy electrons. This limited point of view which can only be used as a means for a qualitative understanding of the properties of intermediate valence systems has the further disadvantage that one cannot calculate transport properties. Thermodynamic properties related to the localized states, however, can be calculated with no further simplifications. It is possible to determine the phase diagram for valence transitions, and also different physical properties of the "metallic" and "insulating" phases*: specific heat, magnetic susceptibilities (static and dynamic) and Mössbauer response functions. For some regions of the phase diagram, the magnetic susceptibilities are similar to those expected from an $s-d$ Hamiltonian with antiferromagnetic coupling, the wide band version of which has been studied by Kondo [3].

In Sect. II we set up the model Hamiltonian. It bears

* Comisión Nacional de Energía Atómica

** Universidad Nacional de Cuyo, Comisión Nacional de Energía Atómica

* We have chosen to refer to the highest valence phase as "metallic" and to the lowest valence one as "insulating", as is the case in SmS. However, the model can be applied also to metal-metal phase transitions as in Ce for example.

0340-224X/79/0036/0037/$02.00

some resemblance with the models proposed by de Chatel et al. [4] and by Ghatak [5] but it is different in that it contains the full spectrum of states identifiable in valence fluctuations. In Sect. III we calculate the phase diagram for valence transitions and analyze the effects of mixing; among others, quenching of the spin entropy at intermediate valence. In Sect. IV we calculate the different physical properties. An analysis of the region of validity of the Kondo Hamiltonian is included.

II. The Model

The model Hamiltonian that we set is the simplest one that still contains the essential features of intermediate valence systems. As we shall see, in spite of its simplicity it will allow us to describe: metal-insulator transitions between intermediate valence phase, static and dynamic magnetic susceptibilities, specific heats and quenching of spin entropy.

Our model system consists of:

1) A set of states representing the "conduction band" of energy ε_k and with creation and annihilation operators $c_{k\sigma}^+$, $c_{k\sigma}$ where $\sigma = \pm$ indicates the spin.

2) A set of "localized states" with a Coulomb repulsion between electrons of opposite spin. These states have single particle energy E_0, creation and annihilation operators b_σ^+, b_σ.

3) An effective repulsion, between localized and conduction electrons at the same site. The most obvious origin for this repulsion is coulombian as pointed out by Falicov and Kimball [6], but in principle there might be other contributions of elastic origin [7]. This term will be treated in the Hartree-Fock approximation from the outset*.

4) A mixing term which hybridizes "localized" and "band" states, and, as we shall see, is essential for the Kondo-like behaviour of the metallic phase properties as well as for the non-integer occupation of the localized states. The Hamiltonian reads

$$H = H_1 + H_2 + H_3 + H_4 \tag{1}$$

where

$$H_1 = \sum_{k\sigma} \varepsilon_{k\sigma} c_{k\sigma}^+ c_{k\sigma} = \sum_{ij} T_{ij} c_{i\sigma}^+ c_{j\sigma} \tag{2}$$

is the Hamiltonian of the conduction band.

* As it will be seen later, we will consider an approach in which the Hamiltonian gets separated in single site Hamiltonians. Clearly, the in-site Coulomb repulsions U and G can be treated exactly in this case and no cooperative effects can be expected. However, we will carry on using the Hartee-Fock approximation in G as a means of simulating more realistic approaches to the problem because our aim here is not to evaluate the role that the different interactions play in producing the phase change, but rather to illustrate the way in which correlation (as produced by U) and hybridization modify the phase diagram.

Here $c_{j\sigma} = \frac{1}{N^{1/2}} \sum_k e^{i\mathbf{k}\cdot\mathbf{R}_j} c_{k\sigma}$, where N is the number of lattice sites and $\mathbf{R}_j$ the coordinate of the j^{th} lattice point.

$$H_2 = \sum_{j\sigma} \left[E_0 b_{j\sigma}^+ b_{j\sigma} + \frac{U}{2} b_{j\sigma}^+ b_{j\sigma} b_{j\sigma}^+ b_{j\sigma} \right] \tag{3}$$

describes the localized states. U is the intra atomic Coulomb repulsion.

$$H_3 = G \sum_{j\sigma\sigma'} (\langle b_{j\sigma}^+ b_{j\sigma} \rangle c_{j\sigma'}^+ c_{j\sigma'} + \langle c_{j\sigma}^+ c_{j\sigma} \rangle b_{j\sigma'}^+ b_{j\sigma'} - \langle b_{j\sigma'}^+ b_{j\sigma'} \rangle \langle c_{j\sigma}^+ c_{j\sigma} \rangle) \tag{4}$$

describes the localized-to-band repulsion term in the Hartree-Fock approximation. $\langle \ldots \rangle$ indicates a thermal average.

$$H_4 = \sum_{j\sigma} V (b_{j\sigma}^+ c_{j\sigma} + c_{j\sigma}^+ b_{j\sigma}) \tag{5}$$

corresponds to the hybridization term, which for simplicity was taken to mix localized and extended states at the same site.

As pointed out by Gonçalves da Silva and Falicov [8] the approximation of taking a conduction band of zero width does not affect the metal-insulator transition predicted by the Hamiltonian (1) within the Hartree-Fock scheme [9]. In what follows we shall make this approximation i.e., $\varepsilon_{k\sigma} \equiv \varepsilon_0$ for all k's. This will leave us with an exactly solvable model. As we shall see below this model Hamiltonian still retains the Kondo-like and intermediate valence characteristics of real systems.

Dropping the now irrelevant site subscript, the model Hamiltonian reduces to

$$H = \sum_\sigma \left[\varepsilon c_\sigma^+ c_\sigma + E b_\sigma^+ b_\sigma + \frac{U}{2} b_\sigma^+ b_\sigma \cdot b_\sigma^+ b_\sigma + V (c_\sigma^+ b_\sigma + b_{\sigma}^+ c_\sigma) \right] - G n n' \tag{6}$$

where $\varepsilon = \varepsilon_0 + G n'$, $E = E_0 + G n$, $n' = \sum_\sigma \langle b_\sigma^+ b_\sigma \rangle$ and $n = \sum_\sigma \langle c_\sigma^+ c_\sigma \rangle$.

We will study the thermodynamic properties of this model Hamiltonian within the canonical ensemble and in the case in which there are two particles per site, which corresponds to the most interesting physical situation. The parameters will be chosen such that $U \to \infty$ while $E + U$ remains finite and of the order of ε. The reason for this choice lies in the fact that it will allow us to go from an insulating phase where the localized states are doubly occupied and thus are non-magnetic, to a metallic phase in which there is

approximately one electron in the localized state and one in the "band".
This situation is similar to that found in the Sm chalcogenides. Another possibility which allows us to go from an empty localized state to a singly occupied highly correlated localized state, as in the case in Ce compounds is to take $U \to \infty$, and $E \sim \varepsilon$.
The relevant basis states are thus the following six:

$$|1\rangle = b_\uparrow^+ b_\downarrow^+ |0\rangle$$
$$|2\rangle = \frac{1}{\sqrt{2}}(c_\downarrow^+ b_\uparrow^+ - c_\uparrow^+ b_\downarrow^+)|0\rangle$$
$$|3\rangle = c_\uparrow^+ b_\uparrow^+ |0\rangle$$
$$|4\rangle = \frac{1}{\sqrt{2}}(c_\downarrow^+ b_\uparrow^+ + c_\uparrow^+ b_\downarrow^+)|0\rangle$$
$$|5\rangle = c_\downarrow^+ b_\downarrow^+ |0\rangle$$
$$|6\rangle = c_\uparrow^+ c_\downarrow^+ |0\rangle \qquad (7)$$

which diagonalize the number of localized and band electrons and simultaneously the total spin.
State $|1\rangle$ corresponds to double occupancy of the localized state, and to zero total spin; state $|2\rangle$ is a singlet ($S=0$) corresponding to one electron in each state. State $|3\rangle$, $|4\rangle$ and $|5\rangle$ form a spin triplet ($S=1$) and also correspond to one electron in each state. State $|6\rangle$ describes double occupancy of the "band". Our choice of parameters ($U \to \infty$, $E+U \sim \varepsilon$) allows us to project state $|6\rangle$ out of the subspace of interest. Of the remaining states, the hybridization term in (6) mixes $|1\rangle$ and $|2\rangle$. This mixing is the origin of the non-integer occupation and of the non-divergence of the static magnetic susceptibility as $T \to 0$ in the metallic phase.

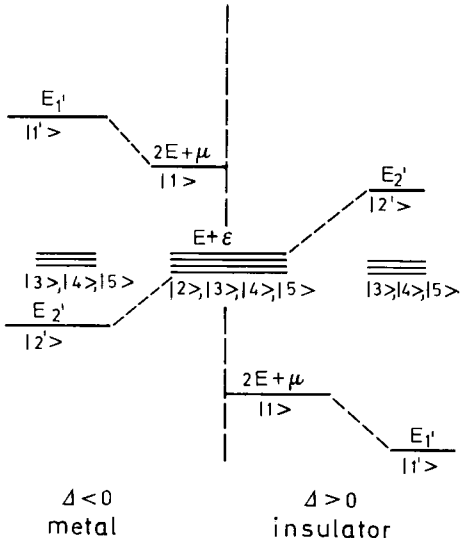

Fig. 1. Level scheme for the metallic and insulating phases. The central part of the drawing corresponds to the level scheme for $V=0$. State $|1\rangle$ is above or below the other quartet according to whether Δ is negative or positive. The further splitting is due to the mixing V

Table 1

Eigenstate	Spin S	S_z	E_i', Eigenenergies $-(E+\varepsilon)$
$\|1'\rangle = \cos\theta\|1\rangle + \sin\theta\|2\rangle$	0	0	$-\frac{1}{2}[\Delta + \text{sign}(\Delta)R]$
$\|2'\rangle = \cos\theta\|2\rangle - \sin\theta\|1\rangle$	0	0	$-\frac{1}{2}[\Delta - \text{sign}(\Delta)R]$
$\|3'\rangle = \|3\rangle$	1	1	0
$\|4'\rangle = \|4\rangle$	1	0	0
$\|5'\rangle = \|5\rangle$	1	−1	0

$$R = \sqrt{\Delta^2 + 8V^2}, \quad \Delta = \varepsilon - E - U; \quad \text{tgn}\,\theta = -\frac{\sqrt{2}V}{E_1' - (E+\varepsilon)}$$

The structure of the energy levels is depicted in Fig. 1 both in the insulating and in the metallic phases. The eigenstates and eigenenergies are given in Table 1.
As it can be seen from Table 1 the ground state is given by $|1'\rangle$ for $\Delta > 0$ and by $|2'\rangle$ for $\Delta < 0$. We identify the insulating phase as having $|1'\rangle$ as the ground state and the metallic phase as having $|2'\rangle$ as the ground state, since as $V \to 0$, $|1'\rangle$ goes into $|1\rangle$ and $|2'\rangle$ into $|2\rangle$.
In the metallic phase $|2'\rangle$, which is a singlet, plays the role of the Kondo ground state. We shall identify $\frac{1}{2}(R+\Delta)$, which is the gap between the singlet ground state and the triplet, with Kondo's J parameter.

III. Phase Diagram

In order to study the thermodynamic properties of the model, we need to evaluate the partition function. This can be easily done using Table 1. The condition $n+n'=2$ can be used to eliminate n'. The result is

$$Z = (3 + e^{-E_1'/T} + e^{-E_2'/T})\, e^{\frac{G}{T}(2-n)n}. \qquad (8)$$

We can define a bare gap Δ_0 through $\Delta = \Delta_0 - 2Gn$ so that $\Delta_0 = \varepsilon_0 - E_0 - U + G$.
The free energy is given by

$$F = -T\ln Z = -2Gn + Gn^2 - T\ln\left(3 + 2e^{\frac{\Delta}{2T}}\cosh\frac{R}{2T}\right). \qquad (9)$$

Minimization of $F(n)$ with respect to n allows us to calculate the equilibrium value of n for different values of the parameters Δ_0, G, V and T.
The equation for n is

$$n = 1 - \frac{\cosh\frac{R}{2T} + \frac{\Delta}{R}\sinh\frac{R}{2T}}{3e^{-\Delta/2T} + 2\cosh\frac{R}{2T}}. \qquad (10)$$

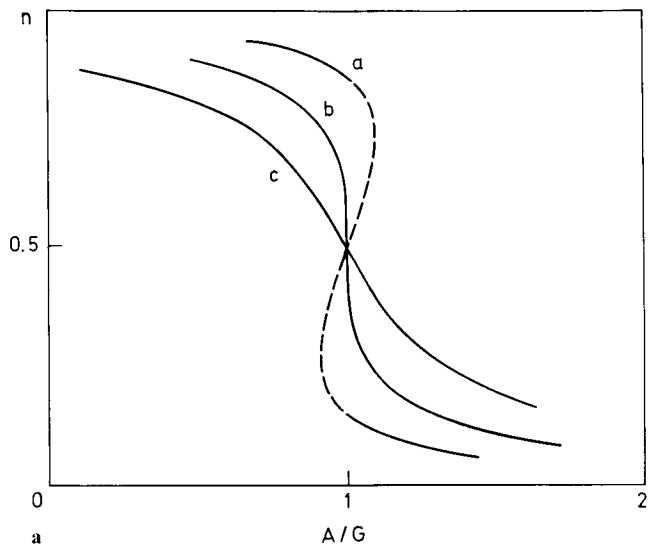

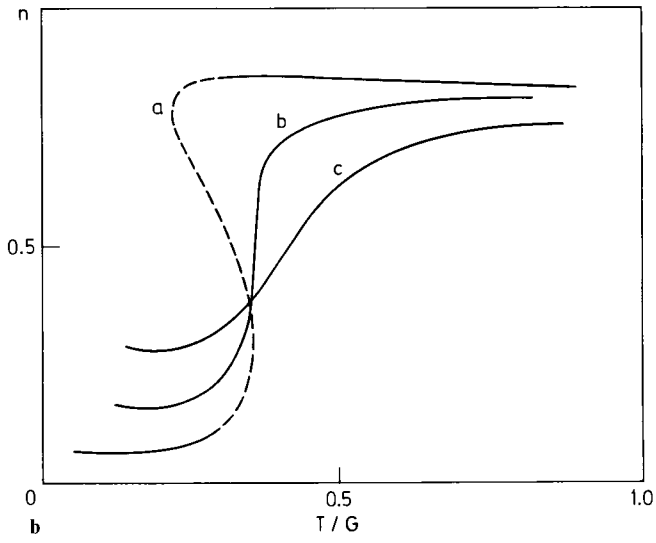

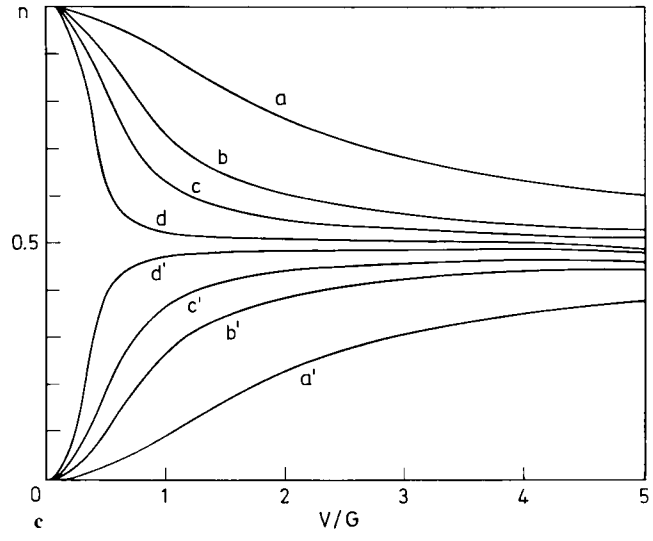

Fig. 2. a Number of conduction electrons n as function of Δ_0/G, at zero temperature, and for different values of V/G. Curve a ($V/G=0.25$) corresponds to a first order transition. Curve b ($V/G=V_c/G=1/\sqrt{8}$) corresponds to a critical transition. Curve c corresponds to a supercritical value of V ($V/G=0.5$). **b** Number of conduction electrons n as function of temperature for $\Delta_0/G=1.4$. Curve a corresponds to a first order transition ($V/G=0.25$) Curves b and c correspond to supercritical transitions ($V/G=0.4$, 0.6). **c** n as a function of V/G for $T=0$ and different values of Δ_0/G. Curves corresponding to Δ_0/G which are equidistant from $\Delta_0/G=1$ lie symmetrically located with respect to $n=1$ 2. Curves a and a' are for $\Delta_0/G=-2$ and 4; b and b' correspond to $\Delta_0/G=0$ and 2; c and c' to 0.5 and 1.5 and d and d' to 0.9 and 1.1

Figure 2a shows the behaviour of n as a function of Δ_0/G, for $T=0$ and different values of V/G. We see that, as was the case in Refs. 2 and 7, the system undergoes continuous or discontinuous variation of n as a function of Δ_0. This would correspond to the variation of n with pressure in real systems [7a, b, 10]. The transitions are between intermediate valence states even at $T=0$.

Figure 2b shows the variation of n with temperature for different values of V/G. Figure 2c gives the behaviour of n for different Δ_0/G.

The phase diagram is drawn in Fig. 3. It can be seen that there is a critical value of V, $V_c=G/\sqrt{8}$, for which the critical temperature vanishes so that for larger values of V there are no more first order transitions [2, 7].

An important feature of these phase diagrams is the fact that for finite V the slope of the curve separating

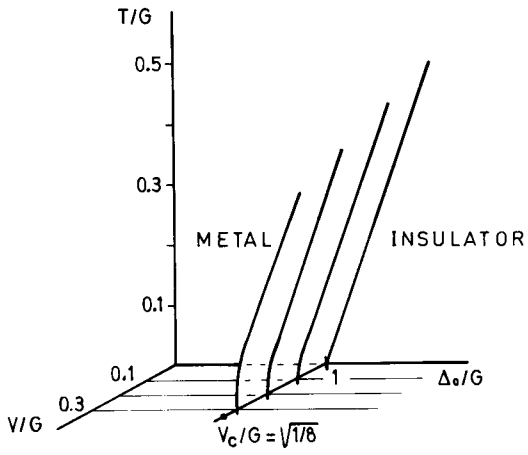

Fig. 3. Phase diagram of model system. The line separating both phases at $T=0$ lies parallel to the V axis; the dot indicates the critical value of V, beyond which there are no more first order transitions

the two phases is infinite at $T=0$ and remains large for $T<J$. At higher temperatures the curves bend down to a slope almost equal to that for $V=0$. The Clausius-Clapeyron formula implies thus that the entropy in both phases is almost the same at low temperatures. Looking at Fig. 1 one can see that this is connected with the fact that a finite V gives a singlet ground state for both phases, thus quenching the spin entropy of the localized spin (Kondo state).

IV. Physical Properties

Specific Heat

From the free energy, Eq. (9), it is easy to calculate the specific heat. Figure 4a shows the temperature dependence in the metallic phase for different values of the mixing parameter V. It is seen that two maxima show up at different temperatures.

Looking at the level scheme in Fig. 1, one can identify the first maximum as due to thermal excitation from the singlet Kondo state to the triplet state. In the Kondo model one would associate this first maximum to the Kondo temperature T_K. The second maximum whose position changes only slightly with V is due to the occupation of the state $|1'\rangle$, corresponding to a greater degree of localization.

As long as there is no phase transition, the specific heat in the insulating phase would show a peak at temperatures of the order of Δ_0, corresponding to the promotion of electrons from the ground state $|2'\rangle$ to the other states.

Static Magnetic Susceptibility

To evaluate the static magnetic susceptibility we must study the effect of an external magnetic field on the Hamiltonian (6). To this end we assume the localized states to have a magnetic moment μ, so that the energies of spin up and spin down electrons are split by $2\mu B$. The band states will be assumed to have no magnetic moment, as a mean of simulating the consequences of the Pauli principle in a broad band.

The magnetic field term couples the states $|2\rangle$ and $|4\rangle$. Since in turn the states $|1\rangle$ and $|2\rangle$ are coupled by the hybridization, we have a three by three matrix to be diagonalized.

After some straightforward algebra, the static susceptibility can be written as

$$\chi_0=\left(\frac{\mu^2}{4T}\right)\frac{1}{Z}(4-2T\sum_i a_i e^{-\beta\Omega_i}) \tag{11}$$

where the sum over i runs from 1 to 3 and a_i and Ω_i take on the values

$$\begin{aligned} a_1&=\frac{\Delta}{2V^2} & \Omega_1&=0\\ a_2&=\frac{(R+\Delta)^2}{8RV^2} & \Omega_2&=-\left(\frac{\Delta-R}{2}\right)\\ a_3&=-\frac{(R-V)^2}{8RV^2} & \Omega_3&=-\left(\frac{\Delta+R}{2}\right). \end{aligned} \tag{12}$$

Figure 5a shows the behaviour of χ_0 for the metallic phase. The zero temperature values of the magnetic susceptibility are determined by the mixture induced

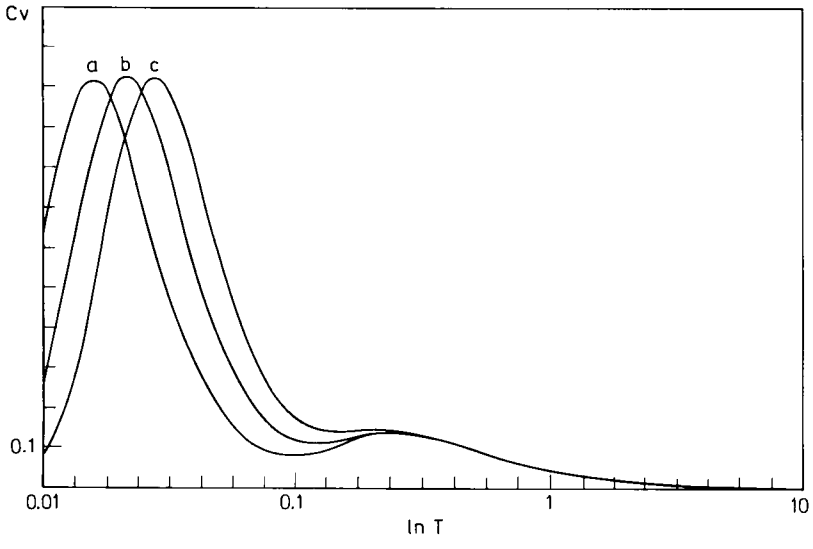

Fig. 4. Specific heats of model system ($k_B=1$) as function of temperature in the "metallic" phase for $\Delta_0/G=-0.5$. Curve a is for $V\,G=0.11$, b for $V/G=0.13$ und c for $V/G=0.15$. The scale on the T axis is logarithmic

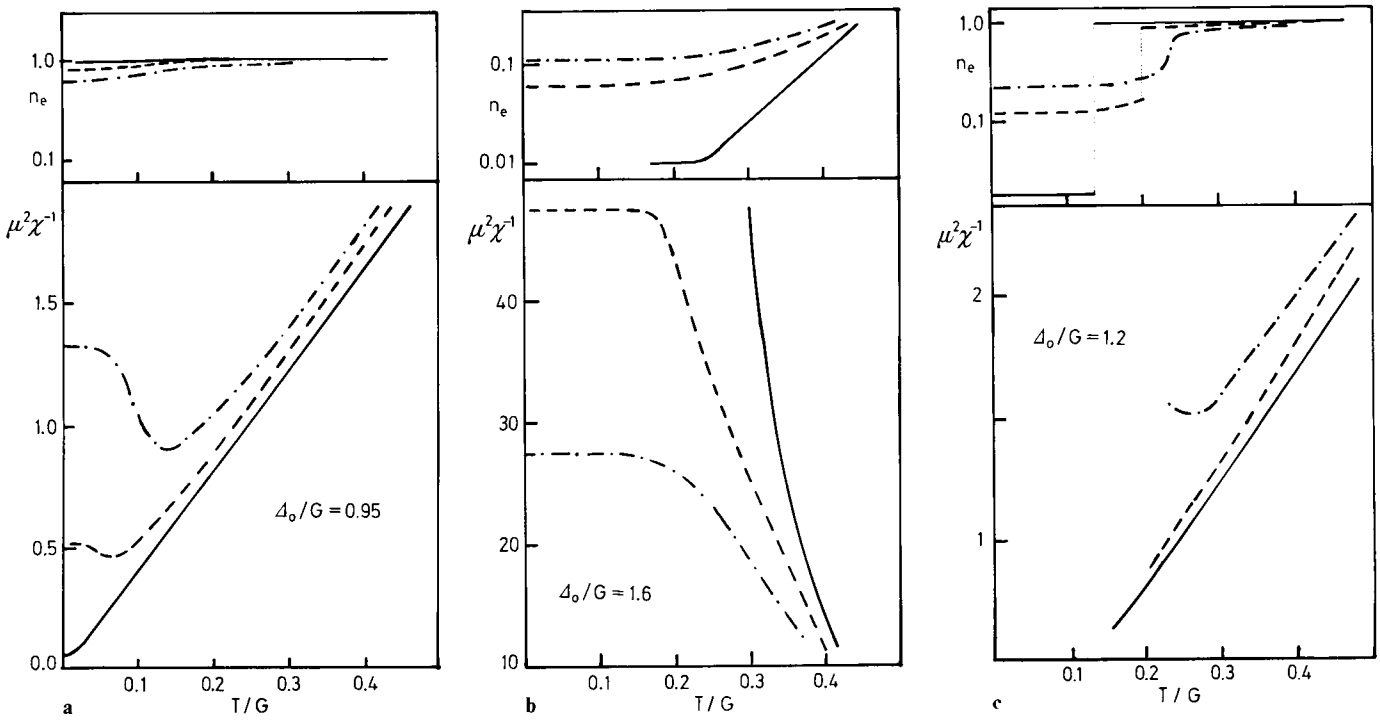

Fig. 5. **a** Inverse static magnetic susceptibility as function of temperature, for $\Delta_0/G = 0.95$ (metallic phase). Full line is for $V/G = 0.1$, dashed line for $V/G = 0.3$ and dot-dashed line for $V/G = 0.4$. Upper part contains a plot of the number of "conduction" electrons per site for the same values of V/G. **b** Inverse static magnetic susceptibility as function of temperature for $\Delta_0/G = 1.6$ (insulating phase). The values of V/G are the same as above. **c** Inverse static magnetic susceptibility for $\Delta_0/G = 1.2$. The three curves correspond to the same three values of V/G as above. The insert for values of n indicates the existence of a first order transition

by the magnetic field between the ground state $|2'\rangle$ and state $|4\rangle$. At temperatures high as compared to their splitting (Kondo temperature) we recover the Curie-Weiss behaviour. Figure 5b corresponds to the insulating phase. The zero temperature value is again determined by the mixture induced by magnetic field between the ground state $|1'\rangle$ and state $|4\rangle$. This mixture is mediated by state $|2\rangle$, thus for small mixing $\left(\frac{V}{\Delta} \ll 1\right)$ the matrix elements go to zero and the susceptibility vanishes. The susceptibility increases with temperature because the probability of having only one electron at the localized site increases. (See inset for values of n.) Finally, Fig. 4c sweeps the transition region. It should be noticed that evaluation of χ_0 requires using the values of n which are to be determined from Eq. (10).

Dynamical Spin Susceptibility

The neutron scattering cross section and other dynamical magnetic properties are given in terms of the correlation function [11]

$$F(\omega) = \frac{1}{2\pi} \int_{-\infty}^{\infty} dt e^{-i\omega t} \langle S^+(0) S^-(t) + S^-(0) S^+(t) \rangle. \quad (13)$$

Where S refers to the localized spin.
The average value appearing in (13) can be explicitly evaluated for this model and we obtain, after a straightforward calculation.

$$\begin{aligned} F(\omega) = {} & P(1') \frac{\sin^2\theta}{4} [\delta(\omega - (E_3 - E_{1'})) + \delta(\omega - (E_5 - E_{1'}))] \\ & + P(2') \frac{\cos^2\theta}{4} [\delta(\omega - (E_3 - E_{2'})) + \delta(\omega - (E_5 - E_{2'}))] \\ & + P(3) \tfrac{1}{4} [\delta(\omega - (E_4 - E_3)) + \sin^2\theta\, \delta(\omega - (E_{1'} - E_3)) \\ & + \cos^2\theta\, \delta(\omega - (E_{2'} - E_3))] \\ & + P(4) \tfrac{1}{4} [\delta(\omega - (E_5 - E_4)) + \delta(\omega - (E_3 - E_4))] \\ & + P(5) \tfrac{1}{4} [\delta(\omega - (E_4 - E_5)) + \sin^2\theta\, \delta(\omega - (E_{1'} - E_5)) \\ & + \cos^2\theta\, \delta(\omega - (E_{2'} - E_5))]. \end{aligned} \quad (14)$$

Here $P(i)$ is the occupation probability for state $|i\rangle$. When no external magnetic field is applied, states $|3\rangle$, $|4\rangle$, and $|5\rangle$ are degenerated and Eq. (14) can be simplified, since $E_3 = E_4 = E_5$ and $P(3) = P(4) = P(5)$. In this situation the neutron spectrum will consist of five peaks located at the energies indicated in the first

Table 2

Poles	Weights
$\omega_0=0$	$\frac{1}{4}[P(3)+2P(4)+P(5)]$
$\omega_1=\frac{1}{2}(\Delta+\text{sign}(\Delta)R)$	$\frac{1}{2}\sin^2\theta P(1')$
$\omega_2=\frac{1}{2}(\Delta-\text{sign}(\Delta)R)$	$\frac{1}{2}\cos^2\theta P(2')$
$-\omega_1$	$\frac{1}{4}\sin^2\theta[P(3)+P(5)]$
$-\omega_2$	$\frac{1}{4}\cos^2\theta[P(3)+P(5)]$

column of Table 2. Their weights are shown in the second column.
The scattering function $F(\omega)$ satisfies the sum rule

$$\int_{-\infty}^{\infty} F(\omega)\,d\omega=\langle S^2\rangle-\langle S_z^2\rangle=\tfrac{2}{3}\langle S^2\rangle. \tag{15}$$

It should be noted that $\langle S^2\rangle$ and $\langle S_z^2\rangle$ above are functions of temperature and of the parameters of the Hamiltonian.
Expression (14) can be seen to verify this sum rule.
The right hand side of (15) can be evaluated straightforwardly to give

$$\langle S_z^2\rangle=\sum_{\mu\nu}P(\mu)|\langle\nu|S_z|\mu\rangle|^2$$
$$=\tfrac{1}{4}[P(1')\sin^2\theta+P(2')\cos^2\theta+P(3)+P(4)+P(5)]. \tag{16}$$

In Fig. 6 we show the position and weight of the peaks as a function of temperature for the insulating phase. It can be seen that at zero temperature only one peak remains. It corresponds to transitions between $|1'\rangle$ and $|3\rangle$ or $|5\rangle$. As the temperature is raised, the intensity of the peak falls down as a consequence of the depopulation of $|1'\rangle$ ($P(1')$ factor in the weight). For further increase in temperature the intensity raises again due to the fact that the mixture increases as the gap is reduced (factor $\sin^2\theta$ in the weight). The peak at $\omega_0=0$ is due to transitions between states $|4\rangle$ and $|3\rangle$ or $|5\rangle$ and its weight is proportional to the population of the triplet. The ω_2 peak corresponds to transitions between $|3\rangle$ or $|5\rangle$ and $|2'\rangle$.

Mössbauer Spectrum

The Mössbauer response of intermediate valence systems has been extensively studied both experimentally [12] and theoretically [13]. The most characteristic feature of this spectrum seems to be the appearance of motional narrowing effects. We will see presently how this fact shows up in our simple model.
To describe the interaction of the nuclear excitations with the intermediate valence system we add to the Hamiltonian the term

$$H_{en}=\omega_1(2-n')a^+a+\omega_2(n'-1)a^+a \tag{17}$$

where $a^+(a)$ is the creation (annihilation) operator for the nuclear excitations. ω_1 is the energy of the nuclear excitation when the electronic system has $n'=1$ and ω_2 the corresponding energy for $n'=2$.
The electromagnetic field of the gamma rays couples to the nuclear excitations through a or a^+ and the Mössbauer spectrum is given according to linear response theory, by

$$M(\omega)=\frac{1}{2\pi}\int_{-\infty}^{\infty}dt\,e^{-i\omega t}\langle a^+(0)a(t)+a(0)a^+(t)\rangle. \tag{18}$$

Here $\langle\ldots\rangle$ includes an average of the nuclear variables over a canonical ensemble and since the energy of the excited states lies in the KeV region we may always consider (18) to be an average over the nuclear ground state. So (18) can be written

$$M(\omega)=\frac{1}{2\pi}\int_{-\infty}^{\infty}dt\,e^{i\omega t}\langle a(t)a^+(0)\rangle. \tag{19}$$

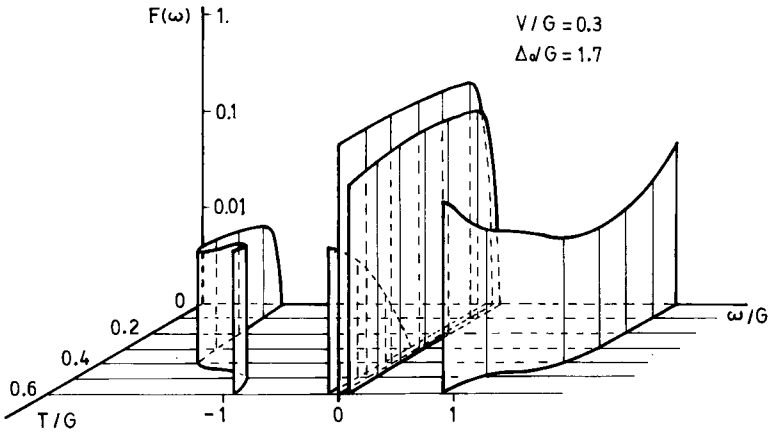

Fig. 6. Position of the poles and weights of the dynamical spin susceptibility $F(\omega)$ as function of temperature. At zero temperature there is only one peak (see text)

To evaluate (19) we can once more use the explicit form of the eigenstates. We must bear in mind that the states that diagonalize $H+H_{en}$ span two mutually orthogonal sets characterized by the eigenvalues of the operator a^+a. For $a^+a=0$, we have the same states as we had before. For $a^+a=1$, we have a new set of states of the same form, but in which the parameter E has to be replaced by $E+\omega_-$, where $\omega_-=\omega_2-\omega_1$. The energies of these new states are shifted by the constant amount $2\omega_1-\omega_2$.
The spectrum can be written as

$$M(\omega)=[P(3)+P(4)+P(5)]\,\delta\left(\omega+\frac{\omega_-}{2}\right)$$

$$+P(1')\left[\cos^2(\theta_1-\theta_0)\,\delta\left(\omega+\frac{\omega_-}{2}-\Omega_{11}\right)\right.$$

$$\left.+\sin^2(\theta_1-\theta_0)\,\delta\left(\omega+\frac{\omega_-}{2}-\Omega_{21}\right)\right]$$

$$+P(2')\left[\sin^2(\theta_1-\theta_0)\,\delta\left(\omega+\frac{\omega_-}{2}-\Omega_{12}\right)\right.$$

$$\left.+\cos^2(\theta_1-\theta_0)\,\delta\left(\omega+\frac{\omega_-}{2}-\Omega_{22}\right)\right]. \tag{20}$$

The quantities θ_0 and θ_1 correspond to the angle θ defined in Table 1, for the different nuclear states. The Ω's are given by

$$\Omega_{11}=E(1,1')-E(0,1')$$
$$\Omega_{12}=E(1,1')-E(0,2')$$
$$\Omega_{21}=E(1,2')-E(0,1')$$
$$\Omega_{22}=E(1,2')-E(0,2').$$

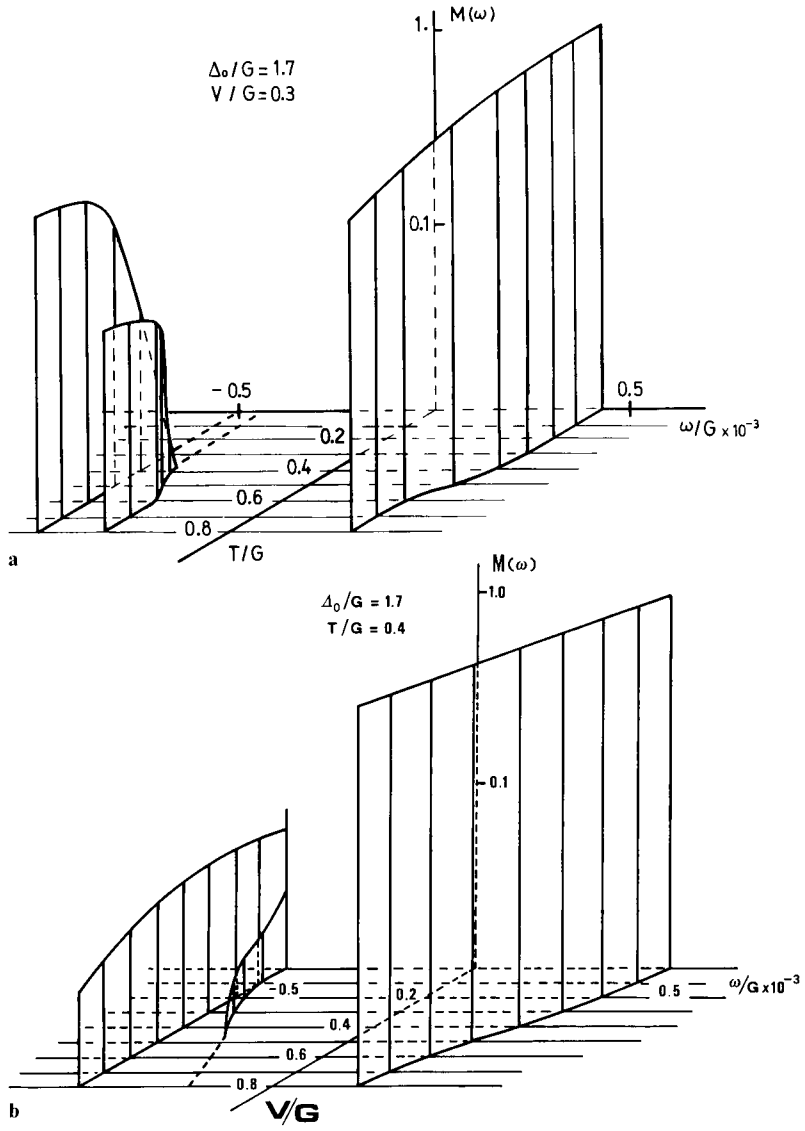

Fig. 7. a Poles and intensities of the Mössbauer response function $M(\omega)$ as function of temperature in the insulating phase. The spectrum is centered around $\frac{\omega_1+\omega_2}{2}$ and the two limiting frequencies correspond to ω_1 and ω_2. The scale factor in terms of G is arbitrary. **b** Poles and intensities of the Mössbauer response function $M(\omega)$ as function of V/G, at finite temperature. It is seen that when V/G is large there will be a single pole at $\frac{\omega_1+\omega_2}{2}$

In the E's the first index corresponds to the nuclear state: the second one, 1′ or 2′, corresponds to the notation of Table 1.

Figure 7a is a plot of the poles and intensities of the Mössbauer response function versus temperature for the insulating phase. It can be seen that at zero temperature, there is only one pole, corresponding to a transition between the ground states of the electronic system associated with the nucleus being in its ground or excited state, respectively. This means transitions between the states $|1, 1'\rangle$ and $|0, 1'\rangle$ for the insulating phase and between $|1, 2'\rangle$ and $|0, 2'\rangle$ for the metallic phase.

As the temperature is raised this pole shifts towards lower frequency values due to the fact that the effective gap Δ has a stronger temperature dependence for the electronic configurations associated with the nuclear ground state, than for the other case. At the same time the corresponding amplitude decreases due to the population of the excited electronic states.

There is another pole, symmetrically located, corresponding to the transitions between the states $|1, 2'\rangle$ and $|0, 2'\rangle$ which has a much smaller amplitude due to the Boltzmann factor.

A third pole, associated to a transition between the two sets of electronic triplet states, shows up at a constant frequency, reflecting the fact that the energies of these states are temperature independent.

There are two other poles related to transitions from $|1, 1'\rangle$ to $|0, 2'\rangle$ and $|1, 2'\rangle$ to $|0, 1'\rangle$ which have much higher energies. Their amplitudes are insignificant due to the sin factors in Eq. (20).

Figure 7b shows the variation of $M(\omega)$ for a fixed temperature as a function of V/G. The three relevant peaks are the same as those of Fig. 7a. It is seen that as V/G increases the transitions between the singlets move towards each other. At the same time the amplitude of the transition between triplets tends to zero. This behaviour resembles the motional narrowing that appears in a more realistic model as one increases the mixing parameters [13].

V. Discussion

The preceding paragraphs show how most of the characteristic features of intermediate valence systems can be understood on the basis of a very simple model. This model shares with real systems what we believe are the essential factors that determine the behaviour of intermediate valence compounds: highly correlated ionic like states, and hibridization between them and s-like uncorrelated states.

As we have seen above, the model can describe phase transitions between intermediate valence phase, non-integer occupation of the correlated states, saturating static magnetic susceptibilities, quasi-elastic peaks in the dynamical magnetic susceptibility and motional narrowing effects in the Mössbauer spectra.

It can be shown that the model properties of the metallic phase for $|\Delta| \gg V$ can be simulated by a narrow band version of the Kondo Hamiltonian $H = J\mathbf{S}\mathbf{s}$ (where $\mathbf{S}$ is the localized spin and $\mathbf{s}$ the "conduction band" spin) identifying J with $\frac{1}{2}(R+\Delta)$. However, many of the properties of the model are not reproduced by the Kondo Hamiltonian. In fact none of the consequences of non-integer occupation (as for example Isomer shifts and weakening of the total intensity of dynamical susceptibilities) can be described in that way. The Schieffer-Wolff transformation can be carried out to all orders in V for this model. The result shows clearly the difference between the Kondo Hamiltonian (based on the second order results) and Hamiltonian (1) needed to describe intermediate valence systems.

Several improvements are necessary to adapt the model to a more realistic and quantitative picture of valence fluctuators; among them:

i) conduction electron hopping between different sites.

ii) more realistic ionic configurations including the level schemes of the intervening $4f$ shells.

iii) phonon variables to correlate lattice vibrations with electron occupancy.

In conclusion, we hope to have proved that quantum admixture and highly correlated ionic states are essential to understand mixed valence phenomena.

This research was supported in part by the OAS Multinational Program for Physics.

References

1. See for example Parks, R.D. (ed.): Valence instabilities and related narrow band phenomena. New York: Plenum Press 1977
2. Leder, H.J., Muhlschlegel, B.: Z. Physik B **29**, 341 (1978); Entel, P., Leder, H.J., Grewe, N.: Z. Physik B **30**, 277 (1978); Entel, P., Leder, H.J. (to be published)
3. Kondo, J.: Progr. Theor. Phys. (Kyoto) **28**, 846 (1962)
4. de Chatel, P.F., Aarts, J., Klaasse, J.C.P.: Comm. Phys. **2**, 151 (1977)
5. Ghatak, S.K.: Physica (1976)
6. Falicov, L.M., Kimball, J.C.: Phys. Rev. Lett. **22**, 997 (1969)
7. a) Alascio, B., López, A.: Solid state Commun. **15**, 1933 (1974)
   b) Wio, H.S., Alascio, B., López, A.: Solid State Commun. **15**, 1933 (1974)
   c) Anderson, P.W., Chui, S.T.: Phys. Rev. B. **9**, 3229 (1974)
8. Gonçalves da Silva, C.E.T., Falicov, L.M.: Solid State Commun. **17**, 1521 (1975)

9. Plischke, M.: Phys. Rev. Lett. **28**. 361 (1972). Gonçalves da Silva, C.E.T., Falicov, L.M.: J. Phys. C. **5**, 906 (1972)
10. Pohl, D.W.: In: Valence Instabilities and Related Narrow Band Phenomena, Parks, R. (ed.). New York: Plenum Press 1977 and references therein
11. Kittel, C.: Quantum Theory of Solids. New York: John Wiley and Sons 1964
12. Coey, J.M.D., Massenet, O.: In: Valence Instabilities and Related Narrow Band Phenomena, Parks, R.D. (ed.). New York: Plenum Press 1977
13. Balseiro, C., Alascio, B., López, A.: Phys. Rev. B (to be published)

B. Alascio
Centro Atómico Bariloche
Comisión Nacional de Energía Atómica
8400 S.C. de Bariloche, R.N.
Argentina

H. Wio
A. López
Universidad Nacional de Cuyo
Comisión Nacional de Energía Atómica
8400 S.C. de Bariloche, R.N.
Argentina